scattering of light by certain crystals," *Sov. Phys.—Solid State,* vol. 12, p. 1157, 1970.
[10] C. C. Wang and E. L. Baardsen, "Study of optical third harmonic generation in reflection," *Phys. Rev.*, vol. 185, p. 1079, 1969; also *Phys. Rev. B,* vol. 1, p. 2827, 1970.
[11] J. J. Wynne and G. D. Boyd, "Study of optical difference mixing in Ge and Si using a CO_2 gas laser," *Appl. Phys. Lett.*, vol. 12, p. 191, 1968.
[12] A. Owyoung, "Ellipse rotation studies in laser host materials," *IEEE Quantum Electron.*, vol. QE-9, pp. 1064–1069, Nov. 1973.
[13] C. R. Giuliano and J. H. Marburger, "Observations of moving self-foci in sapphire," *Phys. Rev. Lett.*, vol. 27, pp. 905–908, 1970.
[14] D. W. Fradin, "The measurement of self-focusing parameters using intrinsic optical damage," *IEEE J. Quantum Electron.* (Corresp.), vol. QE-9, pp. 954–956, Sept. 1973.

Pulse Evolution in Mode-Locked Quasi-Continuous Lasers

GEOFFREY H. C. NEW

***Abstract*—Various models of a passively mode-locked quasi-continuous laser are discussed and the evolution of pulses in various cavity configurations is traced. In certain circumstances, the combined action of amplifier and absorber saturation is shown to lead to rapid pulse compression even when the pulse duration is far shorter than the relaxation time of either nonlinear component. The results are in good agreement with recent streak-camera measurements involving the pulsed rhodamine 6G dye laser and satisfactorily explain the efficient generation of picosecond pulses in CW dye-laser systems. The same pulse-compression mechanism can probably be used to generate ultrashort pulses in other quasi-continuous lasers.**

I. Introduction

VARIOUS authors have demonstrated that the passively mode-locked rhodamine 6G dye laser is a reliable source of picosecond pulses [1]–[8]. The development of mode locking is extremely rapid [9] and the pulses which ultimately evolve are much shorter than the recovery time of the saturable dye most commonly employed [10]–[13].[1] These properties contrast markedly with those of passively mode-locked solid-state systems. Here the mode-locking process typically takes hundreds of cavity transits to develop [15]–[19], and it is generally accepted that the duration of the pulses finally generated is not substantially less than the relaxation time of the saturable absorber [20]–[27].

It was proposed in an earlier paper [28] (hereafter referred to as I) that the striking behavior of the dye laser results from its different dynamic properties and in particular the short (~5-ns) recovery time of the amplifying medium [29]. This ensures that equilibrium is quickly established between the cavity radiation and the population inversion of the rhodamine 6G molecules and, since the transition cross sections of the amplifying and absorbing media are comparable [12], [30], before the growth of mode locking has commenced. For a quasi-continuous system such as this, it was shown in I that amplifier and absorber saturation can in certain circumstances combine to effect pulse shortening even when the pulse duration is far less than either relaxation time. In the giant-pulse solid-state systems, a steady state of this type is never established. The recovery of the amplifier population inversion is so slow that once depleted the gain never recovers. Mode locking takes place during the growth of the giant pulse, and the key to reliable pulse selection is to ensure that the time the intensity distribution takes to pass through the region of maximum absorber discrimination is sufficiently long [15]–[18]. In principle, this can be achieved solely by operating the laser system very close to threshold [15], [31], although Glenn [16], [17] has shown that in practice gain saturation plays a crucial role in slowing the growth rate of the signal through the region of maximum selectivity.

Although gain saturation is thus clearly implicated in the mode-locking process in both types of laser, its role in each case is very different. In the solid-state systems, the saturable absorber is entirely responsible for pulse selection, although the gain saturation helps indirectly by holding the developing intensity profile within the region of strong absorber discrimination [16], [17]. In the quasi-

Manuscript received August 14, 1973.
The author was with the Department of Pure and Applied Physics, The Queen's University of Belfast, Belfast, Northern Ireland. He is now with the Applied Optics Section, Physics Department, Imperial College, London, England.

[1] A preliminary report of a measurement of the recovery time of 3,3'-diethyoxadicarbocyanine iodide is included [13]. The value obtained is in the range 10–50 ps and is in conflict with the results of [10]–[12]. The discrepancy might arise from a confusion between the aperture time of a saturable shutter and the relaxation time of the molecular transition [14], [10]. In any case, the present theory does not preclude the possibility that fast processes exist, although it is contended that on their own these could not explain the rapid buildup of mode locking which is observed experimentally [9], [32].

continuous systems, however, saturable amplification plays a direct part in pulse selection and, indeed, has the same status as saturable absorption in the mode-locking process.

In I [28], the conditions for short-pulse generation in the quasi-continuous systems were established and the possibility of their realization demonstrated. In the present article, the complete time development of a pulse in these circumstances is traced. As well as confirming the earlier conclusions, the results demonstrate that the rate of pulse shortening is extremely rapid, corresponding in a typical case to a pulsewidth reduction factor of $\sqrt{2}$ every cavity round trip. This is in good agreement with recent experimental data [9], as well as with the results of other theoretical investigations [32]. It contrasts markedly with the slow evolution of mode locking in the solid-state laser systems.

II. Laser Models with Discrete Components

In the previous work [28], the behavior of an optical pulse propagating in the laser cavity arrangement shown in Fig. 1(a) was studied in the regime where the cavity round-trip transit time T_{RT} is comparable with the relaxation time of the amplifying component. The pulse duration T_p was assumed to be short compared with the relaxation times of both the amplifying and absorbing media (T_{1a} and T_{1b}, respectively) so that recovery effects during the pulse transit could be ignored. The further condition that $T_{RT} \gg T_{1b} \gg 2D/c \gtrsim T_p$ implied first that absorber recovery was complete between successive cavity transits, secondly that it was insignificant during the return passage to the nearby mirror, and lastly that overlap effects in the absorber cell could be neglected.

The passage of an optical pulse through a "slow" nonlinear amplifying slab is conveniently analyzed in terms of the dimensionless parameter $j(\tau)$ defined by

$$j(\tau) = \sigma_a \int_{-\infty}^{\tau} F(\tau)\, d\tau \tag{1}$$

where $F(\tau)$ is the photon flux at local time $\tau(= t - x/c)$ and σ_a is the stimulated emission cross section of the medium. The value of j at $\tau = +\infty$ is here abbreviated to j_∞ and called simply the pulse energy. Strictly, j_∞ is the total pulse energy per unit area normalized to the level where the amplifier population inversion is depleted to $1/e$ times its initial value (one photon per amplifier molecule). The relation between the initial i and final f values of $j(\tau)$ is

$$j_f(\tau) = \ln \{1 + \alpha(-\infty)\,[\exp(j_i(\tau)) - 1]\} \tag{2}$$

where $\alpha(-\infty)$ is the gain presented to the leading edge of the pulse profile. During the pulse, $\alpha(\tau)$ is a monotonically decreasing function (>1) which determines the gain delivered to the profile as a function of local time

$$\alpha(\tau) = \alpha(-\infty)\exp\{j_i(\tau) - j_f(\tau)\}. \tag{3}$$

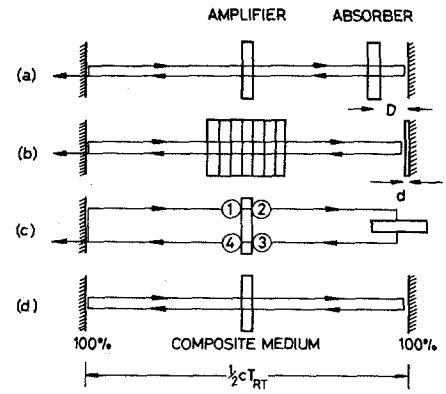

Fig. 1. Laser cavity models. (a) The amplifier is in the center of the cavity and the absorber is separated from the mirror. This system was treated in I for the case where $2D \ll cT_{1b}$ (see Fig. 10). (b) The absorber is in a thin cell in optical contact with one of the cavity mirrors. The amplifier occupies an extended region in the center of the cavity and is shown divided into a number of elements, each of which should be treated separately. As explained in the text, this latter refinement is not employed in the present calculations. (c) The discrete model studied in Sections II and IV. As drawn, the amplifier lies in the center of the cavity, although the problem can be solved for other amplifier positions (see Fig. 12). The single one-way transit through the absorber cell has the same effect on the optical pulse as the contacted cell in (b) provided the absorption cross section is twice as big in the single transit case [see (4)]. Without the factor of 2, this configuration is essentially equivalent to case (a) when $2D \gg cT_{1b}$. The numbers 1–4 appear in the equations describing this model which are listed in the Appendix. (d) The artificial model studied in Section III in which all the amplifying and absorbing components are combined into a single composite element in the center of the cavity.

The gain presented to the extreme trailing edge is $\alpha(+\infty)$, and α subsequently recovers towards the fully pumped level at a rate controlled by the relaxation time T_{1a}.

For a pulse in an absorbing slab, the results are entirely analogous. The loss factor $\beta(\tau)$ is a monotonically increasing function (<1) during the pulse, and returns to its small-signal value after the pulse has passed at a rate determined by the relaxation time T_{1b}. The expression for $j(\tau)$ in (1) must be replaced by one containing the absorption cross section σ_b instead of σ_a. Rather than defining a directly parallel quantity, it is more convenient to use the product $s \times j(\tau)$ for the dimensionless energy in absorbing elements. The obvious definition for s is just σ_b/σ_a although a more general expression is introduced in (4).

By employing the propagation equations for the nonlinear media at $\tau = \pm\infty$, introducing appropriate linear losses, and allowing for incomplete amplifier recovery between pulse transits, it was shown in I that for any cavity configuration above threshold, there exists a unique equilibrium value for j_∞ at every point in the system. Furthermore, under easily realizable conditions, the overall round-trip transmission factors for the extreme leading and trailing edges of the pulse (g_L and g_T, respectively) can both be less than unity. Since the pulse is then confined at both ends while its total energy (j_∞) is constant, its duration must necessarily shorten. In the present paper, the same type of calculation is performed at intermediate values of τ as well, thereby allowing the complete temporal development of the pulse profile to be followed.

In pulsed dye lasers where the evolution of mode lock-

ing has been studied experimentally [9], the saturable absorber solution is regularly contained in a thin cell in optical contact with the adjacent mirror, as shown on the right of Fig. 1(b) [2]–[6], [9], [24]. For the purposes of comparison, it is therefore desirable to introduce an absorber model which applies to this situation. Fortunately, the contacted dye-cell case is easily treated provided the cell is very thin compared with the pulse length (and $T_p \ll T_{1b}$ as before); for it is easy to show that the effect on the pulse is exactly the same as for a single one-way passage through a cell with the same small-signal absorption *but with double the absorption cross section.* The physical reason is that, since only half as many dye molecules are required to produce a given $\beta(-\infty)$ in the two-way as in the one-way case, the contacted cell system is twice as easily saturated. The model shown in Fig. 1(c) is therefore adopted and the general expression for s written

$$s = k \frac{A_a \sigma_b}{A_b \sigma_a} \tag{4}$$

where $k = 2$ for the contacted cell as discussed above. The inclusion of A_a and A_b which are, respectively, the beam areas in the amplifying and absorbing media, allows for telescoping which is employed in some experimental systems to increase the value of s [7], [8]. It should be noted that with $k = 1$, the same model applies to the separated cell arrangement of Fig. 1(a) when $2D \gg cT_{1b}$.

The models of Fig. 1(a) and (c) can be criticized on the grounds that in real laser systems, the amplifying medium extends over a significant region of the laser cavity. Since the energy increases as the pulse progresses, those parts of the amplifier which the pulse reaches later are saturated to a greater extent. Furthermore, different recovery times apply at different positions, and for points away from the cavity center the time delay depends on whether the pulse is towards the left-hand or the right-hand mirror. These complications may be taken into account by dividing the amplifier into a number of slabs as shown in Fig. 1(b) and treating each one separately. However, the results differ only marginally from those obtained with the single thin-slab model and the refinement is therefore not used in any of the present calculations.

III. Pulse Evolution in an Artificial Cavity Model

In the model discussed in the previous section, the various components are arranged in the cavity in discrete blocks as in a real laser system. The discrete model allows pulse development to be traced in almost any cavity configuration and the results are presented in Section IV. However, the complete system of equations is complicated and the processes governing pulse evolution therefore tend to be obscured. In this section, an artificial model is studied which, for the particular case where the amplifier is in the center of the cavity, turns out to have remarkably similar properties to the analogous discrete system. The mathematics is relatively simple, and the approach provides invaluable insight into the pulse-compression mechanism.

In the new model which is shown in Fig. 1(d), all the amplifying and absorbing components (including linear losses) are uniformly distributed in a single cell of thickness d situated at the center of the cavity formed between two 100-percent mirrors. The propagation of a pulse in the composite medium is controlled by the equation

$$\left(\frac{\partial F}{\partial x'}\right)_\tau = (A - B - \Gamma)F = GF. \tag{5}$$

The parameters A and B stand for $n_a\sigma_a$ and $-n_b\sigma_b$, respectively, where n_a and n_b are the population densities in the amplifying and absorbing components, and Γ is the absorption coefficient associated with the linear losses. The amplification coefficient A is related to α, the corresponding amplification factor per round trip by $\alpha = \exp(2dA)$; similar relations define β and γ, the nonlinear and the linear loss factors, respectively.[2] The overall unsaturated gain factor per round trip is

$$g_0 = \alpha_0\beta_0\gamma = \exp 2(A_0 - B_0 - \Gamma) \tag{6}$$

in which d has been set equal to unity and the subscripts 0 distinguish the small-signal values of the saturable parameters. Note that $g_0 = 1$ defines threshold.

Under the influence of an intense pulse, A and B are monotonically decreasing functions of $j(\tau)$, and the gain coefficient G in (5) is given by

$$G(j) = A_i \exp(-j) - B_0 \exp(-sj) - \Gamma. \tag{7}$$

The initial nonlinear absorption coefficient is here taken as the small-signal value which is appropriate if $T_{1b} \ll \frac{1}{2}T_{RT}$. However, A_i is assumed to be less than A_0 as a result of the incomplete recovery of the population inversion between successive pulse transits.

Two conditions define the equilibrium state where the total pulse energy j_∞ maintains the same value everywhere in the cavity. The first condition ensures that the initial amplification coefficient of the composite medium is the same before every pulse transit, by requiring that the final value $A_i \exp(-j_\infty)$ recovers to exactly A_i in the time $\frac{1}{2}T_{RT}$. It is easy to show that the equilibrium value of A_i is

$$A_{i,e}(j_\infty) = \frac{A_0(1 - E)}{(1 - E \exp(-j_\infty))} \tag{8}$$

where

$$E = \exp(-\tfrac{1}{2}T_{RT}/T_{1a}) = \exp(-\tfrac{1}{2}\xi). \tag{9}$$

The parameter ξ defined here is proportional to the cavity length. The second equilibrium condition is that j_∞

[2] $\beta = \exp(-2dB)$; $\gamma = \exp(-2d\Gamma)$.

remains constant as the pulse propagates in the composite medium. The general expression for the variation of $j(\tau)$ with distance is

$$\left(\frac{\partial j}{\partial x'}\right)_\tau = \int_0^{j(\tau)} G(j')\, dj' = I(j) \tag{10}$$

so the requirement is clearly that $I(j_\infty) = 0$. By performing the integration in (10) with A_{ie} substituted for A_i in (7), a transcendental equation is obtained whose single nonzero root is the total pulse energy,

$$A_{ie}(j_\infty) - H(j_\infty) = 0 \tag{11}$$

where

$$H(j_\infty) = \frac{B_0 s^{-1}\{1 - \exp(-sj_\infty)\} + \Gamma j_\infty}{\{1 - \exp(-j_\infty)\}}. \tag{12}$$

Once j_∞ is known, the transmission coefficient $G(j)$ for $j < j_\infty$ can be found from

$$G(j) = A_{ie}(j_\infty)\exp(-j) - B_0 \exp(-sj) - \Gamma. \tag{13}$$

In general $G(j)$ does not represent the gain or loss at any particular point on the pulse profile because $j(\tau)$ varies as the pulse evolves; there is in other words no simple equation to parallel (3) for a single component medium and hence no easy way to trace the details of pulse development using the composite medium model. However, far out on the leading and trailing edges of the pulse envelope, the values of j are approximately constant and the expression for G can then be applied directly. For the leading edge,

$$G_L = G(0) = A_{ie}(j_\infty) - B_0 - \Gamma \tag{14}$$

and for the trailing edge,

$$G_T = G(j_\infty) = A_{ie}(j_\infty)\exp(-j_\infty) - B_0 \exp(-sj_\infty) - \Gamma. \tag{15}$$

The corresponding gain factors per round trip are $g_L = \exp(2G_L)$ and $g_T = \exp(2G_T)$ by analogy with (6). Both g_L and g_T cannot exceed unity (G_L and G_T both > 0) at the same time as (11) is satisfied, but all the other three combinations of positive and negative values can occur. The case where both gain factors are less than unity is of special interest because this defines the situation where pulse compression takes place.

It is clear from (8) and (11) that to realize a particular j_∞ [and hence a particular function $G(j)$], there is a degree of freedom with A_0 and E, or equivalently with g_0 and ξ. The contours of equal j_∞ in the $g_0 - \xi$ plane are easily obtained by combining (6), (8), and (11),

$$\ln g_0 = 2\left[\frac{H(j_\infty)\{1 - E\exp(-j_\infty)\}}{(1 - E)} - B_0 - \Gamma\right] \tag{16}$$

where E is related to ξ through (9). The two particular contours for which $g_L = 1$ or $g_T = 1$ mark the boundaries of the pulse-compression region. The corresponding values of j_∞ follow from (14), (15), and (11). For $g_L = 1$, j_∞ is the root of

$$H(j_\infty) - B_0 - \Gamma = 0 \tag{17}$$

while for $g_T = 1$, j_∞ is the root of

$$H(j_\infty)\exp(-j_\infty) - B_0 \exp(-sj_\infty) - \Gamma = 0. \tag{18}$$

In Fig. 2 pairs of boundary contours are shown for four values of s in the case where

$$\beta_0 = 0.2 \text{ (20-percent small-signal absorber transmission; } B_0 = 0.805)$$
$$\gamma = 0.4 \text{ (60-percent linear losses; } \Gamma = 0.458). \tag{19}$$

(These values of β_0 and γ are employed in all the examples studied in this paper.) For each value of s in Fig. 2, the right- and left-hand contours mark the leading and trailing edge boundaries, respectively, and the region in between is where compression occurs. The value of j_∞ on each contour is given in the figure caption and the variation of j_∞ across the horizontal line $g_0 = 2$ in Fig. 2 is shown in Fig. 3 for various values of s. As s is reduced, there finally comes a point where the value of j_∞ obtained from (17) and (18) goes to zero and for lower values of s no compression region exists. The minimum value of s can be found by expanding the exponentials in (17) and (18) as far as the cubic term in j_∞. In both cases it transpires that j_∞ tends to zero at

$$s_{\min} = \frac{B_0 + \Gamma}{B_0} \tag{20}$$

which, from (19), is 1.569 in the present case. The boundary contours for $s = 1.58$ just above the minimum value are shown in Fig. 2.

In Fig. 4, the function $G(j)$ is plotted for $s = 10$, $g_0 = 2$, and for various values of ξ; an analogous set of curves for $s = 5$ is shown in Fig. 5. The vertical line at the right-hand end of each curve marks j_∞, where the total area under the graph is zero according to the condition $I(j_\infty) = 0$ [(10)]. For the highest and lowest value of ξ in both figures (the longest and shortest cavities), G_L and G_T are, respectively, greater than zero. In all the other cases, both the leading and trailing edge gain coefficients are negative so the conditions for pulse compression are satisfied. The very important feature now emerges that, in these circumstances, there is always an intermediate energy j_p ($0 < j_p < j_\infty$) for which the area under the graph $G(j)$ is also zero ($I(j_p) = 0$). The value of j_p which is marked on the relevant curves in Figs. 4 and 5 is the root of the equation

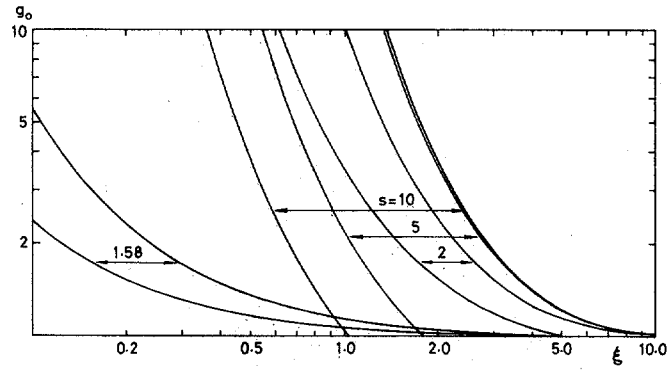

Fig. 2. Boundaries of the pulse compression region in the $g_0 - \xi$ plane for the case where $\beta_0 = 0.2$ and $\gamma = 0.4$ and the amplifier is in the center of the cavity. The parameter g_0 is the small-signal gain [(6)] and $\xi = T_{RT}/T_{1a}$, [(9)]. The results obtained with the discrete and artificial models are so similar that this diagram serves equally well in either case. For each value of s, the right- and left-hand lines are, respectively, the boundaries for the leading edge ($g_L = 1$) and the trailing edge ($g_T = 1$) of the pulse and the region in between is where compression occurs. For the artificial model, the boundaries are exactly coincident with the contours of pulse energy. For $s = 10$, the values of j_∞ on the left- and right-hand lines are 0.530 and 2.306, respectively; for $s = 5$, the values are $j_\infty = 0.664$ and 2.051; for $s = 2$, the values are $j_\infty = 0.430$ and 0.916; and for $s = 1.58$, just above the minimum set by (20), the values are $j_\infty = 0.018$ and 0.035.

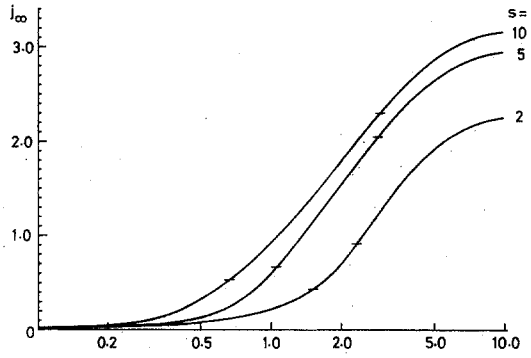

Fig. 3. Pulse energy j_∞ as a function of ξ across the horizontal line $g_0 = 2$ in Fig. 2 for three values of s. The markings on the lines show the boundaries of the pulse compression region and correspond to the values of j_∞ listed in the caption of Fig. 2.

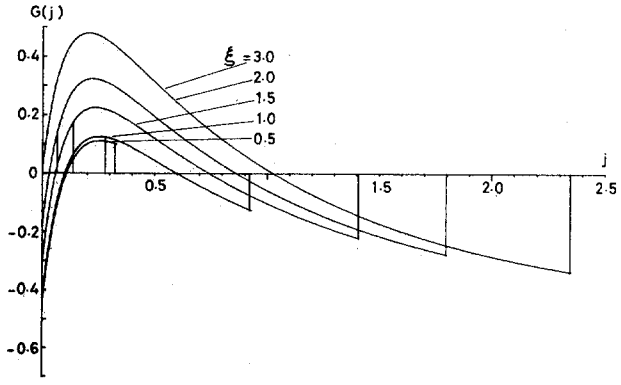

Fig. 4. The transmission coefficient $G(j)$ as a function of j for $s = 10$ and five values of ξ. The vertical lines at the right-hand end of each curve mark the values of j_∞. For the three middle values of ξ, $G(0)$ and $G(j_\infty)$ are both negative and the criteria for pulse compression are therefore satisfied. The additional markings on these three curves show the values of j_p [see (21)], which is the energy contained by the pulse in front of the point where the peak develops. The growth coefficient of the peak is $G(j_p)$.

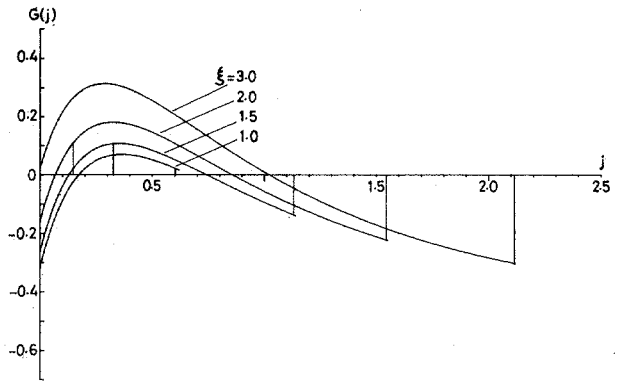

Fig. 5. The analogous set of curves to that in Fig. 4 for $s = 5$. Pulse compression occurs for the middle two of the four values of ξ. Note that in general the absolute magnitude of the transmission coefficient is less than in Fig. 4, which indicates that pulse evolution is less rapid for this lower value of s.

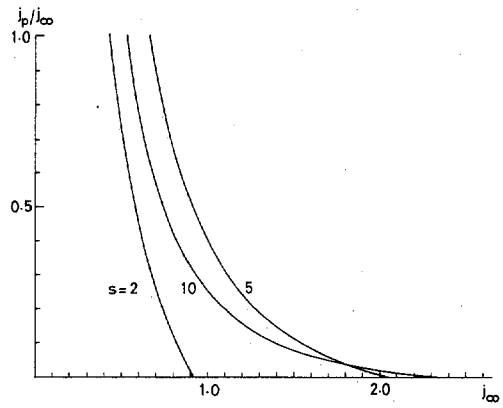

Fig. 6. The ratio j_p/j_∞ as a function of j_∞ for three values of s over the range of pulse energies for which compression occurs.

$$A_{1e}(j_\infty) - H(j_p) = 0 \tag{21}$$

which is just (11) with j_∞ replaced by j_p in H but not in A_{1e}. The meaning of this result is that at the unique point in local time τ_p ($j(\tau_p) \equiv j_p$), the portions of the total pulse energy to the front ($= j_p$) and to the rear ($= j_\infty - j_p$) both remain constant as the profile evolves. As noted earlier in the discussion following (13), $G(j)$ does not generally define the transmission coefficient at particular points in local time. Because $j(\tau_p)$ is constant, however, the point τ_p is an exception and it is here that the peak of the compressed pulse develops. The rate of growth is controlled by $G(j_p)$, which is of course always positive. Whether the peak emerges nearer the front or the rear of the original profile depends on j_p/j_∞ and this ratio is plotted in Fig. 6 for three values of s, over the range of values of j_∞ for which compression takes place. It is clear from Fig. 6 that the point of growth is very sensitive to a small change in the pulse energy caused either by an alteration in the cavity length or in the pumping level. The round-trip growth factor can be seen from Figs. 4 and 5 to be of the order g_T^{-1} except for very low values of j_p/j_∞ where it approximates to g_L^{-1}. These features of the pulse-compression process will be

demonstrated in the treatment of the discrete model given in the next section.

IV. Pulse Compression in the Discrete Model

The complete system of equations describing the discrete model of Fig. 1(c) is listed in the Appendix where the method of solution is also discussed. Throughout this section it is assumed that β_0 (the unsaturated nonlinear loss factor) equals 0.2 and that γ (the total linear loss factor per round trip) equals 0.4, as in (19). The apportionment of the linear losses within the cavity is detailed in (34), although the results are very insensitive to the distribution chosen. The case where the amplifier is positioned at the center of the cavity is examined first. The problem can be solved at $\tau = \pm\infty$ as in I and the boundaries of the pulse compression zone in the $g_0 - \xi$ plane obtained for comparison with Fig. 2 above. However, the boundaries turn out to be so close to those which apply to the analogous artificial model that Fig. 2 is perfectly acceptable for the discrete case also.[3]

The evolution of the pulse profile can be followed by solving the equations at a range of values of the local time. The choice of the initial pulse shape is an important one for reasons that are now discussed. Basov, Letokhov, *et al.* [33], [25]–[36], [41] have studied pulse propagation in composite media exhibiting only nonlinear amplification and linear absorption when amplifier recovery is neglected ($T_{1a} \gg T_p$).[4] The criteria determining pulse development which were established by these authors [35], [41] can be shown to be equivalent to conditions involving the sign of the parameter η defined by

$$\eta = \frac{\partial^2}{\partial \tau^2} \{\ln F(\tau)\}. \tag{22}$$

When η is negative, a pulse shortens even though there is only one "slow" nonlinear process in operation; in the terminology of Icsevgi and Lamb [43] the pulse then has "compact support." A pulse evolving in a mode-locked laser never possesses this special property since there are always points ahead of and behind it where $(\partial/\partial\tau)F(\tau) = 0$. The small fluctuations beyond these minima can potentially "steal" the energy of the main pulse unless they are repressed. Both g_L and g_T must be less than unity if the ideally mode-locked situation is to be reached and maintained, but only one of these parameters need be less than unity for the compression of a pulse with compact support. (This is demonstrated in Fig. 9.) To illustrate the mechanism discussed in the present article, it is clearly inappropriate to start with a Gaussian profile since $\eta < 0$ in this case. A Lorentzian pulse ($\eta > 0$) is, however, a perfectly suitable choice since it does not possess compact support and spreads out as it propagates unless contained at both ends.

Fig. 7 shows the development of a Lorentzian pulse in a laser system operating at $g_0 = 2$, $\xi = 1$, and $s = 10$, which is well inside the compression zone. After the initial transient has been absorbed, the pulse envelope begins to shorten rapidly, the pulse duration roughly halving every two round trips. Note that the time scale in Fig. 7 is arbitrary provided the rate equation approximation and the other assumptions discussed in Section II are satisfied.

Suppose now that the contacted dye cell is removed from the mirror and placed sufficiently far away that $2D \gg cT_{1b}$ in Fig. 1(a). According to (4), the effective value of s drops from 10 to 5, and from Fig. 2 the operating point $g_0 = 2$, and $\xi = 1$ now lies to the left of the trailing-edge boundary. The very different pulse evolution in this case is shown in Fig. 8. Since the trailing-edge gain factor is now greater than unity, the pulse energy spills out at the rear and pulse compression does not occur. The misleading consequences of starting with a Gaussian profile are seen in Fig. 9 where the conditions are in every other respect the same as those in Fig. 8. Despite the value of g_T in excess of unity, the compact support property of the Gaussian pulse restrains the trailing edge and causes the envelope to shorten nevertheless.

Increasing the cavity length in Fig. 8 restores the system to a pulse-compression regime, although the rate of pulse narrowing is in general considerably slower than with $s = 10$, as can be judged by comparing the values of $G(j_p)$ in Figs. 4 and 5. The same observation applies if the separated dye cell is very close to the mirror ($2D \ll cT_{1b}$) which was the assumption made in I. Fig. 10 illustrates the relatively slow pulse compression in this case, for an operating point well within the compression zone.

The process of pulse compression is unaffected if the initial pulse contains complicated internal structure. The selection and subsequent narrowing of a single fluctuation from within a burst of random noise is shown in Fig. 11(a) where the operating conditions are the same as those in Fig. 7. Results obtained from the artificial model explain why the peak of the compressed pulse emerges towards the front of the original profile in Figs. 7 and 11(a), for with the specified parameter values, (11) and (21) yield $j_\infty = 0.921$ and $j_p/j_\infty = 0.304$, respectively. As noted in Section III, Fig. 6 shows that j_p/j_∞ is strongly dependent on j_∞ and that a slight reduction in the pulse energy resulting from a small drop in either g_0 or ξ moves the growth point to later local times. For a 20-percent decrease in the cavity length ($\xi = 0.8$), (11) and (21) yield $j_\infty = 0.697$ and $j_p/j_\infty = 0.567$, and in Fig. 11(b) where the pulse evolution in the

[3] Owing to the asymmetry of the cavity configuration of Fig. 1(c), the compression boundaries do not now exactly coincide with the contours of j_∞ at any point in the system. However, the variation of j_∞ along each boundary is only about 1 percent, and the average j_∞ at locations 1, 2, 3, and 4 in Fig. 1(c) is within a few percent of the value obtained from (11).

[4] In a series of papers [33], [34], [37]–[42] the same authors have investigated both experimentally and theoretically the propagation of optical pulses in media containing *two* nonlinear components. The pulse-shaping mechanisms should, however, be carefully distinguished from those considered in the present article because the Russian authors invariably assume T_{1b} to be short and T_{1a} to be infinitely long (ruby and Nd:glass media were employed in the experiments). In most of the theoretical papers, gain saturation in the composite medium was neglected.

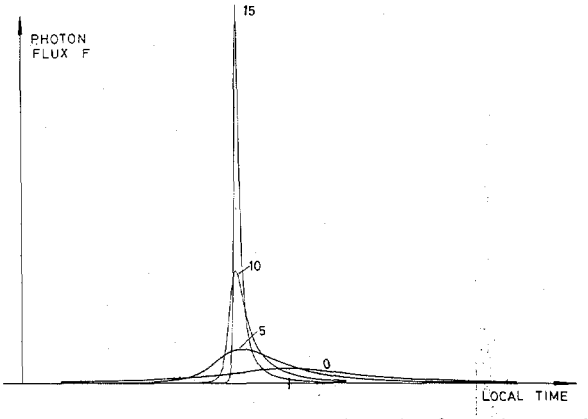

Fig. 7. Compression of an initially Lorentzian pulse after various numbers of round trips in the model of Fig. 1(c) with the amplifier in the center of the cavity. The operating point is $g_0 = 2, \xi = 1$, and $s = 10$ and, as in all cases in this paper, $\beta_0 = 0.2$ and $\gamma = 0.4$. The total pulse energy (the area under the profile) remains constant as the pulse develops. Towards the end of this sequence, the pulse duration is roughly halving every two round trips and this process continues indefinitely until the assumptions on which the model is based break down.

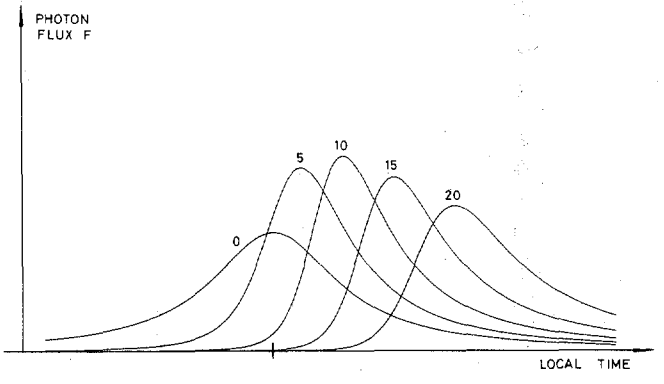

Fig. 8. Pulse evolution with $s = 5$ and all the other conditions the same as in Fig. 7. Because $g_T > 1$ in this case and the Lorentzian profile does not possess compact support, the energy spills out towards the rear and compression does not occur. According to the model, the pulse duration ultimately becomes infinite. In a real laser operating under these conditions, the pulse duration would remain of the same order as the relaxation time of the saturable absorber.

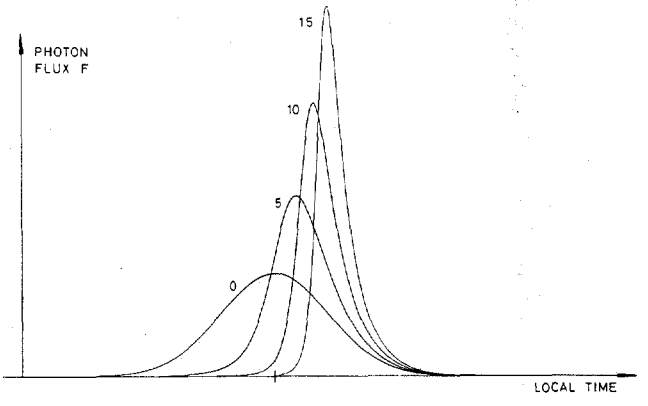

Fig. 9. The evolution of an initially Gaussian pulse under the same conditions as in Fig. 8. The pulse is compressed despite the fact that $g_T > 1$ because of the compact support property of the Gaussian function.

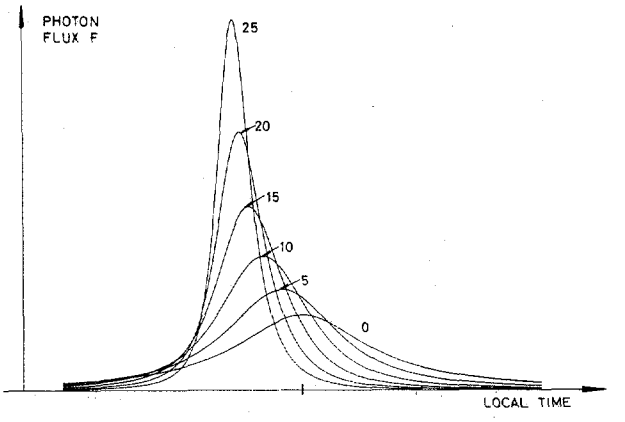

Fig. 10. Compression of an initially Lorentzian pulse in the double transit model of Fig. 1(a) with $2D \ll cT_{1b}$. The parameter values are $g_0 = 1.4, \xi = 1$, and $s = 5$. (See fig. 3 in [28].)

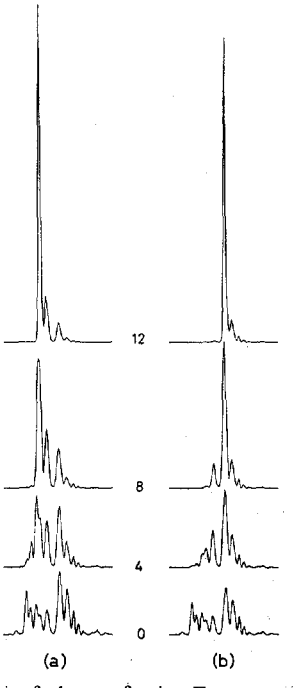

Fig. 11. Compression of a burst of noise. For sequence (a) on the left, the conditions are the same as in Fig. 7 and the growth point of the peak lies towards the front of the original profile as in that figure. To obtain sequence (b) on the right, ξ was reduced from 1.0 to 0.8. The peak now emerges at a later point in local time in agreement with predictions of the artificial model.

analogous discrete model is traced, the maximum correspondingly develops at a later point in local time. The artificial model also predicts a reduction in the growth rate of the pulse maximum from 28 percent to 13 percent per round trip as a result of the shorter cavity, a feature which can also be seen in Fig. 11. The theoretical profiles of Fig. 11 bear a striking similarity to the experimental profiles presented in [9].[5]

All the results presented so far apply to a laser where the

[5] It should be noted that the vertical scale of the profiles in [9] is strongly nonlinear, the true half-intensity point being well over halfway up the profiles.

amplifying component is situated in the center of the cavity. In passively mode-locked CW dye lasers, however, the amplifier is commonly placed near one mirror, while the nonlinear absorber is adjacent to the other [7], [8]. At first sight, it might appear that the discrete model could be applied directly to this new configuration simply by changing the two delay-time values as detailed in (36). When this is done, the boundaries of the pulse-compression region for $s = 5$ and 10 are as shown in Fig. 12 which is to be compared with Fig. 2. The most striking difference lies in the form of the leading-edge boundaries, for Fig. 12 suggests that compression occurs substantially above threshold even for very long (indeed infinitely long) cavities. This conclusion is incorrect, however, because Fig. 12 rests on the basic premise that only one pulse is circulating in the cavity. It is essential to examine the criteria which determine the validity of this single-pulse assumption.

Single-pulse operation is stable if there is no way for a small additional probe pulse to circulate in the cavity so that it receives a net energy gain. When the amplifier is adjacent to the left-hand mirror in Fig. 1(c), the condition is that [6]

$$\alpha_{34}(-\infty) < (\beta_0\gamma)^{-1/2}. \tag{23}$$

If the inequality in (23) is not satisfied, a small fluctuation positioned just ahead of the primary pulse can receive sufficient gain in its double transit through the amplifier to overcome the linear and nonlinear losses. This requirement is more stringent than the condition that $g_L < 1$ for the main pulse and it is not satisfied for long cavities. The right hand of the two dotted lines in Fig. 12 marks the limit of the stable single-pulse regime for $s = 10$. The region between this line and the trailing-edge boundary to its left is where the requirements for single-pulse operation and pulse compression are both met. For $s = 5$, however, the two conditions are mutually exclusive since the trailing-edge boundary now lies to the right of the appropriate dotted line and inside the zone where single-pulse operation is unstable. It is not yet clear whether or not stable multiple pulsing develops when single-pulse operation cannot be maintained. If so, it is unlikely that compression occurs for any of the pulses in the cavity.

In the light of the foregoing discussion, it is obviously necessary to question the validity of the single-pulse assumption for the case, studied in the earlier part of this section, where the amplifying component is in the center of the cavity. A simple argument indicates, however, that, provided the system is working within the pulse-compression region, the criterion for single-pulse stability is automatically satisfied. The only point in local time where the net gain exceeds unity is in the immediate vicinity of the peak of the developing ultrashort pulse. The most delicate situation would concern a weak probe pulse placed so that it emerged from the amplifier at location 2 (or 4) in Fig. 1(c) just as the main pulse entered at location 3 (or 1). The energy gain factor for the probe would clearly be the same (actually slightly less than) as that about to be delivered to the leading edge of the main pulse. The same considerations apply under all circumstances for the linear and nonlinear losses. Thus the condition $g_L < 1$ for the main pulse ensures that the probe dies away. It must be conceded that single-pulse stability does not entirely eliminate the possibility of *additional* stable multiple pulsing modes of operation. This question will be examined in a future study.

[6] For notation, see the Appendix.

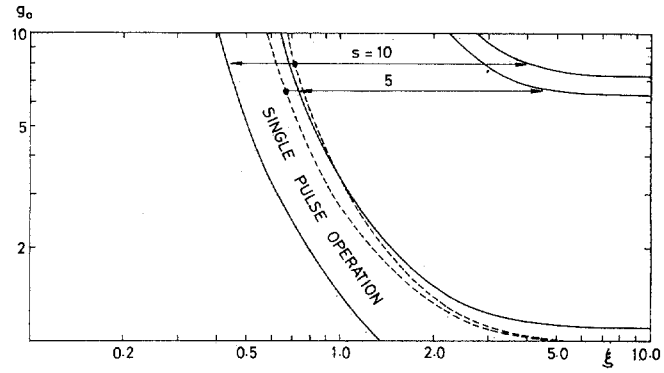

Fig. 12. Boundaries of the pulse-compression region when the amplifier is at the extreme left-hand end of the cavity in the discrete model of Fig. 1(c). The pairs of solid lines are analogous to those in Fig. 2. The situation is, however, more complicated than when the amplifier is in the center of the cavity because for single ultrashort pulse generation, the operating point also has to lie to the left of the appropriate dotted line in this diagram which marks the boundary of the region where single-pulse operation can be maintained. For $s = 10$, the compression zone is therefore much smaller than the solid lines on their own would suggest, while for $s = 5$ the conditions for pulse compression and single-pulse operation are mutually exclusive.

In summary, the conditions for pulse compression are generally more easily realized when the amplifier is at the center of the cavity than when it is at one extreme end. The present theory predicts that in the former case, provided the minimum value of s is exceeded [(20)], a compression regime can always be obtained by judicious adjustment of the pumping level and the cavity length. In the latter case, however, higher values of $s(\gtrsim 6)$ are necessary in order also to satisfy the requirements for single-pulse stability. According to (4), s can be increased by telescoping the beam and by employing a contacted dye cell, and these two experimental techniques may often provide the key to picosecond pulse generation in laser systems of this kind.

V. Conclusion

It has been demonstrated that the generation of picosecond pulses in the mode-locked dye laser does not necessarily imply that the nonlinear absorber exhibits any commensurately short relaxation time. The existence of "fast" processes is not of course ruled out [13], but any explanation of the mode locking on the basis of these alone will need to account for the rapid pulse evolution which has been observed experimentally [9], [32].

When saturable dyes with short recovery times are

employed to mode lock solid-state lasers, the development is notoriously slow. The absorber needs to be "fast" in this case because, being the single nonlinear device, it has to control both edges of the pulse it selects. The situation is different if the single "fast" process is replaced by two "slow" processes. In the dye laser, rapid pulse evolution can occur through the combined action of saturable absorption and saturable amplification, controlling the leading and trailing edges of the pulse profile, respectively. This mechanism adequately explains the experimental results, and is likely to be of importance in other quasi-continuous laser systems.

Further theoretical work is planned, including an examination of the early growth of mode locking from the time when the energy is uniformly distributed in the laser cavity, an investigation of multiple pulsing, and a computer simulation of all stages of pulse evolution.

Appendix

The Equations Describing the Discrete Model of Fig. 1(c)

The complete system of equations describing the model shown in Fig. 1(c) is listed below. The parameters α, β, and γ are, respectively, the amplifier gain and the nonlinear and linear loss factors, and the subscripts 1–4 refer to the locations indicated in Fig. 1(c).

A. Transit 1–2: Amplification

Energy increase:

$$j_2(\tau) = \ln \{1 + \alpha_{12}(-\infty)[\exp(j_1(\tau)) - 1]\}. \tag{24}$$

Profile amplification factor:

$$F_2(\tau) = F_1(\tau)\alpha_{12}(-\infty) \exp [j_1(\tau) - j_2(\tau)]. \tag{25}$$

B. Transit 2–3: Linear and Nonlinear Absorption

Energy decrease:

$$sj_3(\tau) = \gamma_3 \ln \{1 + \beta_0 [\exp(\gamma_2 sj_2(\tau)) - 1]\}. \tag{26}$$

Profile absorption factor:

$$F_3(\tau) = F_2(\tau)\gamma_2\gamma_3\beta_0 \exp [\gamma_2 sj_2(\tau) - sj_3(\tau)/\gamma_3]. \tag{27}$$

(Amplifier recovery):

$$\ln \{\alpha_{34}(-\infty)\} = \tfrac{1}{2}(1 - E_{23}) \ln \alpha_0 + E_{23} \ln \alpha_{12}(+\infty)$$
$$E_{23} = \exp(-t_{23}/T_{1a}) \tag{28}$$

where t_{23} is the pulse transit time between locations 2 and 3. Note that in calculating the amplification factor prior to the pulse transit 3–4, $\ln \alpha_{12}(+\infty)$ is taken to represent the average population inversion in the slab after the transit 1–2. This is a slightly different procedure from that adopted in I.

C. Transit 3–4: Amplification

Energy increase:

$$j_4(\tau) = \ln \{1 + \alpha_{34}(-\infty) [\exp(j_3(\tau)) - 1]\}. \tag{29}$$

Profile amplification factor:

$$F_4(\tau) = F_3(\tau)\alpha_{34}(-\infty) \exp [j_3(\tau) - j_4(\tau)]. \tag{30}$$

D. Transit 4–1: Linear Losses

Energy decrease and profile absorption factor:

$$j_1(\tau) = \gamma_4 j_4(\tau) \tag{31}$$
$$F_1(\tau) = \gamma_4 F_4(\tau). \tag{32}$$

(Amplifier recovery):

$$\ln \{\alpha_{12}(-\infty)\} = \tfrac{1}{2}(1 - E_{41}) \ln \alpha_0 + E_{41} \ln \{\alpha_{34}(+\infty)\}$$
$$E_{41} = \exp(-t_{41}/T_{1a}). \tag{33}$$

The comments following (28) also apply here.

Equations (24), (26), and (29) are analogous to (2) while (25), (27), and (30) are analogous to (3). The problem could in principle be solved by eliminating the variables which would lead to transcendental equations of the type obtained in Section III. In fact, after starting with arbitrary initial values of $j_1(\infty)$ and $\alpha_{12}(-\infty)$, the equations were solved cyclically until the parameters repeated themselves from one round trip to the next. The method of solution thus paralleled the process following the injection of a pulse of arbitrary energy into a real laser system. The pulse envelope shape was then specified and the equations solved from then on for a range of values of the local time τ in order to trace the process of pulse evolution.

The parameter values were similar to those used in Section III [(19)],

$$\beta_0 = 0.2$$
$$\gamma_2 = \gamma_3 = 0.9$$
$$\gamma = \gamma_2\gamma_3\gamma_4 = 0.4. \tag{34}$$

The results were largely unaffected by a change in the distribution of the linear losses between locations 2, 3, and 4.

When the amplifier was centered in the cavity, the delay times employed in (28) and (33) were

$$t_{23} = t_{41} = \tfrac{1}{2}T_{RT} = \tfrac{1}{2}\xi T_{1a}. \tag{35}$$

To obtain Fig. 12, the amplifier was positioned at the extreme left-hand end of the cavity in Fig. 1(c) and the

time delays were then

$$t_{23} = T_{RT}, \qquad t_{41} = 0. \tag{36}$$

Complications which arise with this latter configuration are discussed in the main body of the text.

REFERENCES

[1] W. Schmidt and F. P. Schafer, "Self-mode-locking of dye lasers with saturable absorbers," *Phys. Lett.*, vol. 26A, pp. 558–559, Apr. 1968.

[2] D. J. Bradley and F. O'Neill, "Passive mode-locking of flashlamp-pumped Rhodamine dye lasers," *J. Opt. Electron.*, vol. 1, pp. 69–74, 1969.

[3] D. J. Bradley, A. J. F. Durrant, F. O'Neill, and B. Sutherland, "Picosecond pulses from mode-locked dye lasers," *Phys. Lett.*, vol. 30A, pp. 535–536, Dec. 1969.

[4] D. J. Bradley, B. Liddy, A. G. Roddie, W. Sibbett, and W. E. Sleat, "Direct measurement of duration and background energy content of dye laser picosecond pulses," *Opt. Commun.*, vol. 3, pp. 426–428, Aug. 1971.

[5] E. G. Arthurs, D. J. Bradley, and A. G. Roddie, "Frequency-tunable transform-limited picosecond dye laser pulses," *Appl. Phys. Lett.*, vol. 19, pp. 480–482, Dec. 1971.

[6] ——, "Passive mode-locking of flashlamp-pumped dye lasers tunable between 580 and 700 nm," *Appl. Phys. Lett.*, vol. 20, pp. 125–127, Feb. 1972.

[7] E. P. Ippen, C. V. Shank, and A. Dienes, "Passive mode-locking of the CW dye laser," *Appl. Phys. Lett.*, vol. 21, pp. 348–350, Oct. 1972.

[8] F. O'Neill, "Picosecond pulses from a passively mode-locked CW dye laser," *Opt. Commun.*, vol. 6, pp. 360–363, Dec. 1972.

[9] E. G. Arthurs, D. J. Bradley, and A. G. Roddie, "Build-up of picosecond pulse generation in passively mode-locked Rhodamine dye lasers," *Appl. Phys. Lett.*, vol. 23, pp. 88–89, July 1973.

[10] ——, "Photoisomer generation and absorption relaxation in the mode-locking dye 3,3′-diethyloxadicarbocyanine iodide," *Opt. Commun.*, vol. 8, pp. 118–123, June 1973.

[11] ——, "Picosecond measurement of 3,3′-diethyloxadicarbocyanine iodide and photoiosomer fluorescence," *Chem. Phys. Lett.*, vol. 22, pp. 230–234, Oct. 1973.

[12] D. N. Dempster, T. Morrow, R. Rankin, and G. F. Thompson, "Photochemical characteristics of cyanine dyes: I. 3,3′-diethyloxadicarbocyanine iodide (DODI) and 3,3′-diethylthiadicarbocyanine iodide (DTDI)," *J. Chem. Soc. Faraday II*, vol. 68, pp. 1479–1496, 1972.

[13] G. E. Busch, R. P. Jones, and P. M. Rentzepis, "Picosecond spectroscopy using a picosecond continuum," *Chem. Phys. Lett.*, vol. 18, pp. 178–185, Jan. 1973.

[14] G. Mourou, B. Drouin, and M. M. Denariez-Roberge, "Variable ultrafast photographic shutter," *Appl. Phys. Lett.*, vol. 20, pp. 453–455, June 1972.

[15] B. Ya. Zel'dovich and T. I. Kuznetsova, "Generation of ultrashort light pulses by means of lasers," *Sov. Phys.—Usp.*, vol. 15, pp. 25–44, July–Aug. 1972 (transl. from *Usp. Fiz. Nauk*, vol. 106, pp. 47–84, Jan. 1972).

[16] W. H. Glenn, "Dynamics of mode-locked lasers: A statistical model and experimental results," *IEEE J. Quantum Electron. (1972 Int. Quantum Electronics Conf., Digest of Tech. Papers)*, QE-8, p. 601, June 1972.

[17] ——, "Research investigation of the generation, measurement and properties of picosecond laser pulses," United Aircraft Corp., Rep. L920935-8, June 1972.

[18] P. G. Kryukov and V. S. Letokhov, "Fluctuation mechanism of ultrashort pulse generation by laser with saturable absorber," *IEEE J. Quantum Electron.*, QE-8, pp. 766–782, Oct. 1972.

[19] M. W. McGeoch, "A computational theory of short pulse generation," *Appl. Phys.*, vol. 1, pp. 293–299, 1973.

[20] E. M. Garmire and A. Yariv, "Laser mode-locking with saturable absorbers," *IEEE J. Quantum Electron.*, QE-3, pp. 222–226, June 1967.

[21] J. A. Fleck, "Origin of short pulse emission by passively Q-switched lasers," *J. Appl. Phys.*, vol. 39, pp. 3318–3327, June 1968.

[22] N. G. Basov, P. G. Kriukov, V. S. Letokhov, and Yu. V. Senatskii, "Generation and amplification of ultrashort optical pulses," *IEEE J. Quantum Electron. (Special Issue on 1968 Int. Quantum Electronics Conf.: Part I)*, QE-4, pp. 606–609, Oct. 1968.

[23] V. S. Letokhov, "Generation of ultrashort light pulses in a laser with a nonlinear absorber," *Sov. Phys.—JETP*, vol. 28, pp. 562–568, Mar. 1969 (transl. from *Zh. Eksp. Teor. Fiz.*, vol. 55, pp. 1077–1089, Sept. 1968).

[24] D. J. Bradley, G. H. C. New, and S. J. Caughey, "Relationship between saturable absorber cell length and pulse duration in passively mode-locked lasers," *Opt. Commun.*, vol. 2, pp. 41–44, May–June 1970.

[25] M. A. Duguay, J. W. Hansen, and S. L. Shapiro, "Study of Nd:glass laser radiation," *IEEE J. Quantum Electron.*, QE-6, pp. 725–743, Nov. 1970.

[26] V. I. Malyshev, A. A. Sychev, and V. A. Babenko, "Investigation of the character of the emission of a neodymium glass laser with a passive shutter having a finite relaxation time," *JETP Lett.*, vol. 13, pp. 419–422, June 1971 (transl. from *Pis'ma Zh. Eksp. Teor. Fiz.*, vol. 11, pp. 588–592, June 1971).

[27] V. A. Babenko, V. I. Malyshev, and A. A. Sychev, "Method of reducing the relaxation time of a passive neodymium-glass laser shutter," *JETP Lett.*, vol. 14, pp. 314–317, Oct. 1971 (transl. from *Pis'ma Zh. Eksp. Teor. Fiz.*, vol. 14, pp. 461–465, Oct. 1971).

[28] (Known as I throughout the present article) G. H. C. New, "Mode-locking of quasi-continuous lasers," *Opt. Commun.*, vol. 6, pp. 188–192, Oct. 1972 (*erratum:* The value of ξ used to obtain fig. 3 in this previous paper was 1.0, not 0.75 as stated in the figure caption and in the accompanying text).

[29] J. P. Webb, W. C. McColgin, O. G. Peterson, D. L. Stockman, and J. H. Eberly, "Intersystem crossing rate and triplet state lifetime for a lasing dye," *J. Chem. Phys.*, vol. 53, pp. 4227–4229, Dec. 1970.

[30] O. G. Peterson, J. P. Webb, W. C. McColgin, and J. H. Eberly, "Organic dye laser threshold," *J. Appl. Phys.*, vol. 42, pp. 1917–1928, Apr. 1971.

[31] B. Hausherr, E. Mathieu, and H. Weber, "Influence of saturable-absorber transmission and optical pumping on the reproducibility of passive mode locking," *IEEE J. Quantum Electron.*, QE-9, pp. 445–449, Apr. 1973.

[32] G. H. C. New and D. H. Rea, to be published.

[33] N. G. Basov, R. V. Ambartsumyan, V. S. Zuev, P. G. Kryukov, and V. S. Letokhov, "Nonlinear amplification of light pulses," *Sov. Phys.—JETP*, vol. 23, pp. 16–22, July 1966 (transl. from *Zh. Eksp. Teor. Fiz.*, vol. 50, pp. 23–34, Jan. 1966).

[34] R. V. Ambartsumyan, N. G. Basov, V. S. Zuev, P. G. Kryukov, and V. S. Letokhov, "Propagation of a light pulse in a nonlinearly amplifying and absorbing medium," *JETP Lett.*, vol. 4, pp. 12–14, July 1966 (transl. from *Pis'ma Zh. Eksp. Teor. Fiz.*, vol. 4, pp. 19–22, July 1966).

[35] N. G. Basov and V. S. Letokhov, "Change of light pulse shape by nonlinear amplification," *Sov. Phys.—Dokl.*, vol. 11, pp. 222–224, Sept. 1966 (transl. from *Dokl. Akad. Nauk.*, vol. 167, pp. 73–76, Sept. 1966).

[36] R. V. Ambartsumyan, N. G. Basov, V. S. Zuev, P. G. Kryukov, and V. S. Letokhov, "Short-pulse Q-switched laser with variable pulse length," *IEEE J. Quantum Electron. (1966 Int. Quantum Electronics Conf.)*, QE-2, pp. 436–441, Sept. 1966.

[37] V. S. Letokhov, "Formation of ultrashort pulses of coherent light," *JETP Lett.*, vol. 7, pp. 25–28, Jan. 1968 (transl. from *Pis'ma Zh. Eksp. Teor. Fiz.*, vol. 7, pp. 35–38, Jan. 1968).

[38] N. G. Basov *et al.*, "Fluctuation structure of a giant laser pulse and its variation when passing through a nonlinear absorber," *JETP Lett.*, vol. 9, pp. 256–258, Apr. 1969 (transl. from *Pis'ma Zh. Eksp. Teor. Fiz.*, vol. 9, pp. 428–432, Apr. 1969).

[39] N. G. Basov, P. G. Kryukov, V. S. Letokhov, and Yu. A. Matveets, "Formation of an ultrashort light pulse propagating in a two-component medium," *Sov. Phys.—JETP*, vol. 29, pp. 830–835, Nov. 1969 (transl. from *Zh. Eksp. Teor. Fiz.*, vol. 56, pp. 1546–1556, May 1969).

[40] N. G. Basov, P. G. Kryukov, V. S. Letokhov, Yu. A. Matveets, and S. V. Chekalin, "Amplification of an ultrashort pulse in a two-component medium," *JETP Lett.*, vol. 10, pp. 308–309, Nov. 1969 (transl. from *Pis'ma Zh. Eksp. Teor. Fiz.*, vol. 10, pp. 479–482, Nov. 1969).

[41] P. G. Kryukov and V. S. Letokhov, "Propagation of a light pulse in a resonantly amplifying (absorbing) medium," *Sov. Phys.—Usp.*, vol. 12, pp. 641–670, Oct. 1969 (transl. from *Usp. Fiz. Nauk*, vol. 99, pp. 169–227, Oct. 1969).

[42] P. G. Kryukov, Yu. A. Matveets, S. V. Chekalin, and O. B. Shatverashvili, "Formation of ultrashort laser pulses with the aid of a two-component medium," *JETP Lett.*, vol. 16, pp. 81–83, Aug. 1972 (transl. from *Pis'ma Zh. Eksp. Teor. Fiz.*, vol. 16, pp. 117–120, Aug. 1972).

[43] A. Icsevgi and W. E. Lamb, "Propagation of light pulses in a laser amplifier," *Phys. Rev.*, vol. 185, pp. 517–545, Sept. 1969.